

Biological significance of tumor budding at the invasive front of human colorectal carcinoma cells

YUSRA, SHUHO SEMBA and HIROSHI YOKOZAKI

Division of Pathology, Department of Pathology, Kobe University Graduate School of Medicine, Kobe, Japan

Received January 24, 2012; Accepted April 10, 2012

DOI: 10.3892/ijo.2012.1459

Abstract. At the invasive front of colorectal carcinoma (CRC), the existence of tumor budding (TB), the detachment and migration of small clusters of tumor cells from the neoplastic epithelium, correlates with high incidence of local invasion and distant metastasis; however, the molecular background of TB is still unknown. In human CRC-derived SW480 cells, CD133⁺ cells showed cancer stem cell (CSC)-like properties, high tumorigenicity and pluripotency. By a comparative study of gene expression between CD133⁺ and CD133⁻ SW480 cells, high sensitivity against transforming growth factor- β (TGF- β) was suggested in CD133⁺ SW480 cells. Interestingly, treatment with recombinant TGF- β 1 increased the numbers of cells expressing CD133 and SNAIL. Furthermore, in CD133⁻ SW480 cells, the SNAIL-induced epithelial-mesenchymal transition (EMT) restored the population of CD133⁺ cells and increased tumorigenicity, cell motility/invasiveness and matrix metalloproteinase 2 (MMP2) expression. In stage II CRC tissues, TB was associated with increased levels of SNAIL expression as well as high incidence of metachronous lymph node metastasis post-surgical resection. These findings suggest that TGF- β regulates not only the induction of EMT but also the restoration of CSCs in CRC. The tumor microenvironment at the invasive front is important for the formation of tumor buds in CRC.

Introduction

Tumor budding (TB) initially termed as sprouting, is a morphologic phenomenon observed at the advancing edge of neoplasms and is characterized by isolated or small clusters of tumor cells that detach from the neoplastic epithelium and migrate a short distance into the neoplastic stroma, which may explain the more aggressive behavior of the tumors which show this feature (1,2). In human colorectal carcinoma (CRC), evaluation of TB is therefore a useful prognostic marker (3,4), however, the detailed molecular mechanisms of TB formation remain unknown.

Recently, accumulating evidence has demonstrated that CRC consists of a heterogeneous population of cells and contains a subset of cells that initiate and propagate tumors with high efficiency (5). Since these cells, called cancer stem cells (CSC) or cancer-initiating cells, exhibit not only stem cell properties such as self-renewal and multipotency but also resistance to chemotherapy or radiotherapy (6), there is an urgent need to elucidate the molecular background underlying the maintenance of colorectal CSCs. Numerous colorectal CSC markers have been identified, including Lgr5 (7,8), CD44 (9,10), aldehyde dehydrogenase (ADH) (11) and, most recently, CD133 (12). Indeed, lineage-tracing studies have shown that CD133⁺ cells are located at the base of crypts in the intestine and generate the entire intestinal epithelium, suggesting that CD133⁺ cells are intestinal stem cells and susceptible to transformation into tumors that retain a fraction of mutant CD133⁺ CSCs (13). CD133⁺ colorectal CSCs grew exponentially for more than one year *in vitro* as undifferentiated tumor spheres in serum-free medium, maintaining the ability to engraft and reproduce the same morphological and antigenic pattern of the original tumor (14). A clinicopathological study on CRC reported that patients with high CD133⁺ CSCs had significantly poorer overall survival (15,16).

As described above, TB at the invasive front and CD133⁺ CSCs within the tumor have been established as prognostic markers of human CRC, respectively; nevertheless, the association between TB and CSCs is still unknown. In this study, we investigated the nature of colorectal CSCs and attempted to reproduce TB *in vitro* and *in vivo* to examine whether cells making up tumor buds might have CSC-like properties, or CSCs at the invasive front might form tumor buds.

Materials and methods

Cell culture, magnetic bead separation and gene transfection. Human CRC-derived SW480 cells obtained from American Type Culture Collection (Manassas, VA, USA) were maintained in RPMI-1640 (Invitrogen, Carlsbad, CA, USA) containing 10% fetal bovine serum (FBS; Nichirei, Tokyo, Japan) and antibiotics. For magnetic bead separation, SW480 cells were labeled with anti-CD133 microbeads (Miltenyi, Auburn, CA, USA) and separated on an autoMACS separator (Miltenyi). The human SNAIL-coding region (NM_005985) was subcloned into the pCX4bsr vector to generate pSNAIL as described previously (17). Using effectene transfection reagent (Qiagen, Hilden, Germany), pSNAIL and empty vector (EV) were transduced

Correspondence to: Dr Shuho Semba, Division of Pathology, Department of Pathology, Kobe University Graduate School of Medicine, 7-5-1 Kusunoki-cho, Chuo-ku, Kobe 650-0017, Japan
E-mail: semba@med.kobe-u.ac.jp

Key words: tumor budding, CD133, transforming growth factor- β 1, SNAIL, colorectal carcinoma

into CD133⁺ SW480 cells according to the manufacturer's instruction.

Tumor sphere formation and flow cytometry. Cells were maintained in DMEM/F12 (BD Biosciences, Franklin Lakes, NJ, USA) supplemented with 20 ng/ml of epidermal growth factor (EGF; Sigma, St. Louis, MO, USA), 40 ng/ml of basic fibroblast growth factor (bFGF; Sigma) and 2 ng/ml of transforming growth factor- β 1 (TGF- β 1; Sigma). Tumor spheres were obtained by mixing the cells and Matrigel (BD Biosciences)-containing DMEM/F12 (Invitrogen) and plated on a 4-well chamber slide for more than four weeks. For flow cytometric analysis, cells were washed with phosphate-buffered saline (PBS) and supplemented with anti-human CD133 antibody conjugated with R-phycoerythrin (Miltenyi). The cell pellets were washed with 1% bovine serum albumin (BSA) in PBS and fixed using 1% paraformaldehyde. Expression of CD133 was analyzed using a FACS Calibur cytometer (BD Biosciences).

RT-PCR and quantitative real-time RT-PCR. The primer sets used in this study are listed in Table I. RT-PCR was performed with a One-Step RT-PCR assay kit (Qiagen). Thirty minutes after incubation at 50°C, each 25 μ l reaction mixture containing 10 ng of total RNA was amplified for 30 cycles with the following regimen: denaturation at 94°C for 30 sec; annealing at 58°C for 30 sec and extension at 72°C for 1 min. The products underwent electrophoresis on 2% agarose gel. Quantitative real-time RT-PCR was conducted with an ABI PRISM 7700 Sequence Detection System (Applied Biosystems, Foster City, CA, USA) and QuantiTect SYBR Green RT-PCR kit (Qiagen). The real-time cycler conditions were reverse transcription at 50°C for 30 min, followed by 45 cycles of denaturation at 94°C for 15 sec, annealing at 52°C for 30 sec and elongation at 72°C for 30 sec. The threshold cycle (C_t) was standardized to the sample glyceraldehyde-3-phosphate dehydrogenase (*GAPDH*) value ($\Delta C_t = \text{Gene } C_t - \text{GAPDH } C_t$), and this value was then compared between two kinds of cells using the $\Delta\Delta C_t$ method, which was then used to determine the fold change ($= 2^{[-\Delta\Delta C_t]}$).

Immunofluorescence. Cells and tumor spheres were fixed with 4% paraformaldehyde and then incubated with blocking solution containing 1% BSA. Formalin-fixed and paraffin-embedded tissue sections were also used. The antibodies used are as follows: CD133 (Miltenyi), TGF- β type 1 (TGFBR1; Santa Cruz Biotechnology, Santa Cruz, CA, USA) and type 3 receptors (TGFBR3; Abcam, Cambridge, MA, USA), MUC2 (Santa Cruz Biotechnology), villin (Thermo Scientific, Waltham, MA, USA), MUC5Ac (Santa Cruz Biotechnology), Chromogranin A (CgA; Dako, Glostrup, Denmark), Snail (SNAIL; Abcam), E-cadherin (CDH1; BD Biosciences), vimentin (VIM; Epitomics, Burlingame, CA, USA) and α -smooth muscle actin (SMA; Abcam). Cy2- or Cy3-conjugated antibody against rabbit/mouse IgGs (GE Healthcare, Little Chalfont, UK) were used as secondary antibodies. The nuclei were stained with 4,6-diamidino-2-phenylindole (DAPI).

Tumorigenicity test. Cells (1×10^3 - 10^6 cells/200 μ l Matrigel) were inoculated subcutaneously into the back of 12-week-old severe combined immunodeficiency (SCID) mice (Japan Clea, Tokyo, Japan). Four weeks after inoculation, the mice were

Table I. The primer sets used for RT-PCR and quantitative real-time RT-PCR in this study.

Gene	Sequence
<i>CDX2</i>	F: 5'-GGA ACC TGT GCG AGT GG-3' R: 5'-TTC CTC CGG ATG GTG ATG TA-3'
<i>CD133</i>	F: 5'-GCG TGA TTT CCC AGA AGA TA-3' R: 5'-CCC CAG GAC ACA GCA TAG AA-3'
<i>CD10</i>	F: 5'-ACT CTA TGC AAC CTA CGA TG-3' R: 5'-TGT CAA AGT TGC CGT AAC GG-3'
<i>MUC2</i>	F: 5'-CGA AAC CAC GGC CAC AAC GTC T-3' R: 5'-GAC CAC GGC CCC GTT AAG CA-3'
<i>CD44</i>	F: 5'-CAG TCA CAG ACC TGC CCA ATG-3' R: 5'-AAC CTC CTG AAG TGC TGC TCC-3'
<i>TGFBR1</i>	F: 5'-ATT CCT CGA GAC AGG CCG TT-3' R: 5'-CTG GTC CAG CAA TGA CAG C-3'
<i>TGFBR3</i>	F: 5'-AGT ATG GAG CAG TTA CTT CAT T-3' R: 5'-AGC AAG GTA ATT GAG TGA GAG-3'
<i>CDH1</i>	F: 5'-GCT GGA GAT TAA TCC GGA CA-3' R: 5'-GCT GGC TCA AGT CAA AGT CC-3'
<i>VIM</i>	F: 5'-CTT CGC CAA CTA CAT CGA CA-3' R: 5'-GCT TCA ACG GCA AAG TTC TC-3'
<i>MMP2</i>	F: 5'-ACG ACC GCG ACA AGA AGT AT-3' R: 5'-ATT TGT TGC CCA GGA AAG TG-3'
<i>MMP9</i>	F: 5'-GAC AAG CTC TTC GGC TTC TG-3' R: 5'-TCG CTG GTA CAG GTC GAG TA-3'
<i>GAPDH</i>	F: 5'-TGA TGA CAT CAA GAA GGT GGT GA-3' R: 5'-TCC TTG GAG GCC ATG TGG GCC-3'

F, forward; R, reverse.

sacrificed and paraffin-embedded tumor sections were used for hematoxylin and eosin (H&E) staining and immunohistochemistry (IHC). Initiating cell frequency was calculated using the extreme limiting dilution analysis (ELDA) (18).

cDNA microarray analysis. Total cellular RNA was extracted using RNeasy Mini Kit (Qiagen) according to the manufacturer's recommendations from CD133⁺ and CD133⁻ SW480 cells that were sorted based on their expression for CD133 using autoMACS separator (Miltenyi). The concentration of RNA was determined by measuring the absorbance at 260 nm in a spectrophotometer. A cDNA microarray was performed by Human Expression Array version 2.0 (Agilent Technologies, Palo Alto, CA, USA). The *in vitro* transcription, oligonucleotide array hybridization and scanning were performed according to Takara Bio protocols (Takara Bio, Otsu, Japan). Briefly, double-stranded cDNA was synthesized from total RNA, and was labeled with RNA Fluorescence Labeling Core Kit (Takara Bio). Arrays were then scanned with GeneArray scanner (Agilent Technologies) to obtain image and signal intensities. After data normalization, significance analysis of microarray (SAM) plot

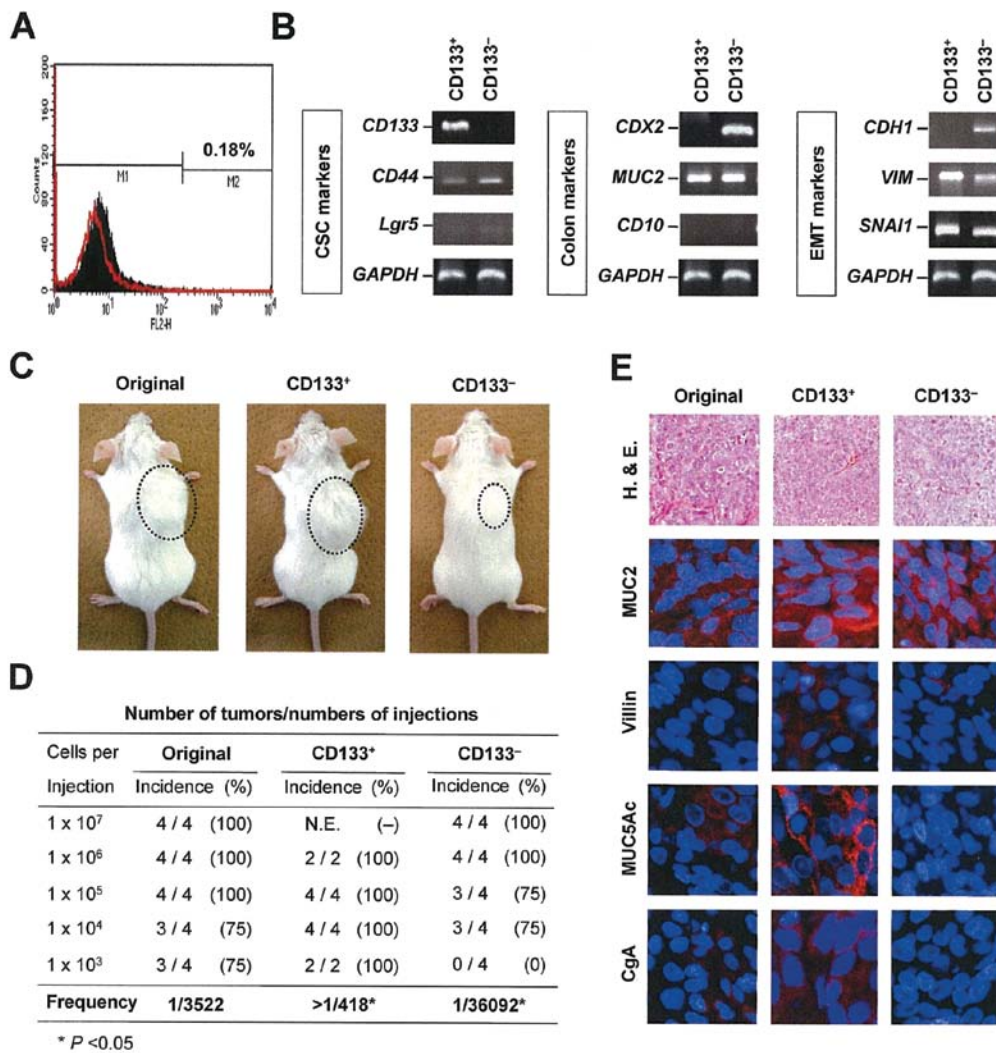


Figure 1. Characteristic of CD133⁺ SW480 cells. (A), Result of flow cytometric analysis. The percentage of CD133⁺ SW480 cells was 0.18%. Red line is the negative control. (B), Expressions of CSC markers (*CD133*, *CD44* and *Lgr5*), colon markers (*CDX2*, *MUC2* and *CD10*) and EMT markers (*CDH1*, *VIM* and *SNAI1*) in CD133⁺ and CD133⁻ SW480 cells. (C), Gross appearance of tumors derived from SW480 cells (original, CD133⁺ and CD133⁻). (D), Results of limiting dilution assay. SW480 cells (original, CD133⁺ and CD133⁻) were inoculated into SCID mice subcutaneously with Matrigel. Initiating cell frequency was calculated using ELDA as described in Materials and methods. Included in calculation, assumption of 100 CD133⁺ cells initiate 0 tumor in 2 injections. (E), IHC of MUC2, villin, MUC5Ac and CgA expressions in tumors derived from SW480 cells (original, CD133⁺ and CD133⁻).

analysis was performed and significantly altered genes were identified in accordance to the manufacturer's protocol (<http://chem.agilent.com>).

Wound healing assay and invasion assay. For the wound healing assay, cultured cells at almost 100% confluence were serum-starved for 12 h. After scratching the monolayer, cells were washed with PBS and then cultured for 24 h. The distance of scratching in 0 h minus in 24 h was measured. Cell invasion activities were estimated using cell culture inserts with an 8- μ m pore size membrane coated with Matrigel. Aliquots of 2.5×10^5 cells were placed in upper chamber with serum-free medium, whereas the lower chamber was loaded with RPMI-1640 containing 10% FBS. After 48-h incubation, the non-invading cells were removed, and the invaded cells on the lower surface of the membrane were counted.

Tissue samples and IHC. A total of 59 formalin-fixed and paraffin-embedded stage II CRC samples obtained from Kobe

University Hospital (Kobe, Japan) were collected. At the time of surgical resection, these cases were diagnosed as stage II CRC; however, metachronous lymph node metastasis was detected in 32 cases of the patients. Informed consent was obtained from all patients and the study was approved by the Kobe University Institutional Review Committee. Statistical analysis was performed using StatView 5.0.1. (SAS, Cary, NC, USA). TB was determined according to the criteria of Ueno *et al* (2). IHC was performed using the labeled streptavidin-biotin kit (Dako) with antibodies against CDX2 (Biogenex, San Ramon, CA, USA) and SNAI1 (Abcam).

Results

CD133 recognizes colorectal CSCs. CD133⁺ cells at the colon crypts are tissue stem cells that differentiate into enterocytes, enteroendocrine cells and goblet cells (7). In CRC-derived SW480 cells, the frequency of CD133⁺ cells was only 0.18% (Fig. 1A); however, there were discrepancies in the expressions

Table II. The genes differentially down-regulated in CD133⁻ SW480 cells in comparison with CD133⁺ SW480 cells.

GDB accession no.	Description	Log2 ratio	Gene symbol
NM_130436	Dual-specificity tyrosine-phosphorylation regulated kinase 1A	-2.63	DYRK1A
NM_007224	Neurexophilin 4	-2.63	NXPH4
NM_003528	Histone cluster 2, H2be	-2.52	HIST2H2BE
NM_019055	Roundabout homolog 4	-2.33	ROBO4
NM_002471	Myosin, heavy chain 6, cardiac muscle, alpha	-2.30	MYH6
NM_013397	Prickle homolog 4	-2.24	PRICKLE4
NM_001926	Defensin, alpha 6	-2.20	DEFA6
NM_004475	Flotillin 2	-2.13	FLOT2
NM_000691	Aldehyde dehydrogenase 3 family, memberA1	-2.11	ALDH3A1
NM_018557	Low density lipoprotein-related protein 1B	-2.06	LRP1B
NM_003865	HESX homeobox 1	-2.03	HESX1
NM_014552	Grainyhead-like 1	-2.01	GRHL1
NM_005376	v-myc homolog 1, lung carcinoma derived	-1.99	MYCL1
NM_031944	Mix1 homeobox-like 1	-1.99	MIXL1
NM_000422	Keratin 17	-1.98	KRT17
NM_152597	Fibrous sheath interacting protein 1	-1.97	FSIP1
NM_001007527	LMBR1 domain containing 2	-1.96	LMBRD2
NM_005503	Amyloid beta precursor protein-binding, family A, member 2	-1.96	APBA2
NM_033297	NLR family, pyrin domain containing 12	-1.95	NLRP12
NM_024325	Zinc finger protein 343	-1.94	ZNF343
NM_003965	Chemokine(C-C motif) receptor-like 2	-1.93	CCRL2
NM_182539	t-complex-associated-testis-expressed 1	-1.91	TCTE1
NM_052910	SLIT and NTRK-like family, member 1	-1.91	SLITRK1
NM_147192	Diencephalon/mesencephalon homeobox 1	-1.91	DMBX1
NM_001781	CD69 molecule	-1.90	CD69
NM_022436	ATP-binding cassette, sub-family G, member 5	-1.90	ABCG5
NM_006613	GRB2-related adaptor protein	-1.90	GRAP
NM_007031	Heat shock transcription factor 2 binding protein	-1.90	HSF2BP
NM_152437	Zinc finger protein 664	-1.90	ZNF664
NM_021200	Pleckstrin homology domain containing, family B, member 1	-1.88	PLEKHB1
NM_004067	Chimerin (chimaerin) 2	-1.88	CHN2
NM_012426	Splicing factor 3b, subunit 3	-1.88	SF3B3
NM_014055	Intraflagellar transport 81 homolog	-1.85	IFT81
NM_000658	Autoimmune regulator	-1.83	AIRE
NM_017659	Glutaminyl-peptide cyclotransferase-like	-1.83	QPCTL
NM_004807	Heparan sulfate 6-O-sulfotransferase 1	-1.82	HS6ST1
NM_172312	Sapiens sperm associated antigen 8	-1.82	SPAG8
NM_014598	Suppressor of cytokine signaling 7	-1.81	SOCS7
NM_138343	Kinesin light chain 4	-1.81	KLC4
NM_014942	Ankyrin repeat domain 6	-1.80	ANKRD6
NM_006983	Matrix metalloproteinase 23B	-1.79	MMP23B
NM_173561	Unc-5 homolog C-like	-1.79	UNC5CL
NM_005276	Glycerol-3-phosphate dehydrogenase 1	-1.79	GPD1
NM_004612	Transforming growth factor, beta receptor 1	-1.78	TGFBR1
NM_001079802	Fukutin	-1.78	FKTN
NM_000419	Integrin, alpha 2b	-1.76	ITGA2B
NM_001032297	Zinc finger protein 658B	-1.76	ZNF658B
NM_198582	Kelch-like 30	-1.76	KLHL30
NM_004403	Deafness, autosomal dominant 5	-1.74	DFNA5
NM_003277	Claudin 5	-1.74	CLDN5
NM_005557	Keratin 16	-1.73	KRT16
NM_017649	Cyclin M2	-1.73	CNNM2

Table II. Continued.

GDB accession no.	Description	Log2 ratio	Gene symbol
NM_001076787	Tumor protein p53 inducible protein 11	-1.73	TP53I11
NM_182983	Hepsin	-1.73	HPN
NM_053017	ADP-ribosyltransferase 5	-1.70	ART5
NM_031431	Component of oligomeric golgi complex 3	-1.70	COG3
NM_022124	Cadherin-like 23	-1.70	CDH23
NM_153282	Hyaluronoglucosaminidase 1	-1.69	HYAL1
NM_203471	Lectin, galactoside-binding, soluble, 14	-1.69	LGALS14
NM_003243	Transforming growth factor, beta receptor III	-1.68	TGFBR3
NM_021603	FXYD domain containing ion transport regulator 2	-1.68	FXYD2
NM_001085	Serpin peptidase inhibitor, clade A, member 3	-1.68	SERPINA3
NM_133467	CBP-interacting transactivator, Glu/Asp-rich C-terminal domain 4	-1.67	CITED4
NM_018207	Tripartite motif-containing 62	-1.67	TRIM62
NM_054028	Acyl-malonyl condensing enzyme 1-like 2	-1.67	AMAC1L2
NM_001312	Cysteine-rich protein 2	-1.65	CRIP2
NM_018334	Leucine rich repeat neuronal 3	-1.65	LRRN3
NM_017525	CDC42 binding protein kinase gamma	-1.64	CDC42BPG
NM_001013706	Lipid storage droplet protein 5	-1.64	LSDP5
NM_005495	Solute carrier family 17, member 4	-1.64	SLC17A4
NM_138576	B-cell CLL/lymphoma 11B	-1.63	BCL11B
NM_173849	Goosecoid homeobox	-1.63	GSC
NM_001518	General transcription factor II, i	-1.62	GTF2I
NM_004851	Napsin A aspartic peptidase	-1.62	NAPSA
NM_001771	CD22 molecule	-1.62	CD22
NM_001782	CD72 molecule	-1.61	CD72
NM_014574	Striatin, calmodulin binding protein 3	-1.60	STRN3
NM_032528	ST6 beta-galactosamide alpha-2,6-sialyltransferase 2	-1.60	ST6GAL2
NM_001011545	BTB and CNC homology 1	-1.60	BACH1
NM_007225	Neurexophilin 3	-1.60	NXPH3
NM_000529	Melanocortin 2 receptor	-1.59	MC2R
NM_016315	GULP, engulfment adaptor PTB domain containing 1	-1.59	GULP1
NM_017576	Kinesin family member 27	-1.59	KIF27
NM_033508	Glucokinase (hexokinase 4)	-1.59	GCK

of the other colorectal CSC markers *CD44* and *Lgr5* (Fig. 1B). Similar results were detected in the other human CRC cell lines (data not shown). We also examined the differential expressions of colon markers (*CDX2*, *MUC2* and *CD10*) and epithelial-mesenchymal transition (EMT) markers (*CDH1*, *VIM* and *SNAIL*) between CD133⁺ and CD133⁻ SW480 cells. Interestingly, CD133⁺ SW480 expressed extremely low levels of *CDX2* and *CDH1*, whereas they expressed higher levels of *VIM* and *SNAIL* (Fig. 1B). These findings suggested that CD133⁺ SW480 cells were characterized by dedifferentiation and EMT.

In addition, CD133⁺ SW480 cells demonstrated high potential as CSCs: the tumorigenicity of CD133⁺ SW480 cells was 86 times higher than that of CD133⁻ SW480 cells (Fig. 1C and D). The xenografts developed in SCID mice showed pluripotency by expressing the enterocyte makers *MUC2* (colon), villin (small intestine), *MUC5Ac* (stomach) as well as the enteroendocrine marker *CgA* (Fig. 1E). Since *CDX2* is a transcription factor that regulates development and

differentiation of the intestinal epithelium (19), we transduced *CDX2*-expression vector (pCDX2) into CD133⁺ SW480 cells as a colorectal CSC differentiation model. Induction of *CDX2* not only promoted cell differentiation and branch formation in three-dimensional culture but also effectively decreased tumorigenicity (unpublished data). Thus, we concluded that CD133 recognizes colorectal CSCs.

TGF-β restores CD133⁺ SW480 cells and induces EMT. To identify genes that are responsible for the maintenance of CSC-like properties, a comparative study of gene expression profiles was performed using CD133⁺ and CD133⁻ SW480 cells (Table II). Among the down-regulated genes (>1.6-fold) in CD133⁻ SW480 cells, we focused on the type 1 (*TGFBR1*) and type 3 (*TGFBR3*) TGF-β receptor genes. We confirmed that expressions of *TGFBR1* and *TGFBR3* in CD133⁺ SW480 cells were higher than those in CD133⁻ cells at the mRNA and protein levels (Fig. 2A and B).

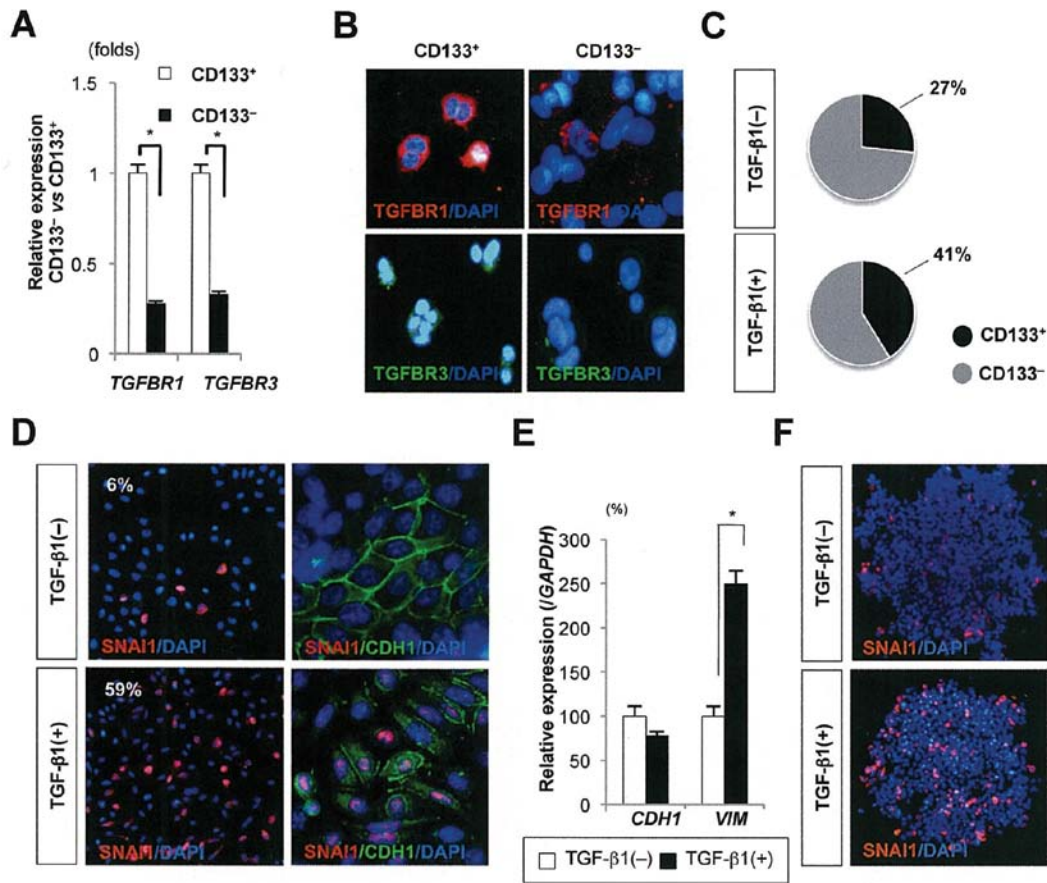


Figure 2. Impact of TGF- β on the maintenance of CSC and EMT in SW480 cells. (A), Relative expression of *TGFBR1* and *TGFBR3* in CD133⁺ cells and CD133⁻ SW480 cells. (B), Immunofluorescence of TGFBR1 and TGFBR3 in SW480 cells. The nuclei were stained with DAPI. (C), Percentages of CD133⁺ cells in CD133⁺ SW480 cells in the presence or absence of TGF- β 1 treatment for 48 h. (D), Altered expression of SNAI1 and CDH1 in SW480 cells by treatment with TGF- β . (E), Relative expressions of *CDH1* and *VIM* in the CD133⁺ cells in the presence or absence of TGF- β treatment. (F), SNAI1 expression in sphere derived from CD133⁺ SW480 cells in the presence or absence of TGF- β treatment.

Based on these results, we hypothesized that CSCs may have high sensitivity to TGF- β . TGF- β and its family members have been implicated in the development and maintenance of stem cells (20) and the induction of EMT (21). Then, we treated CD133⁺ SW480 cells with TGF- β 1 and found that TGF- β 1 maintained the population of CD133⁺ SW480 cells more than in the absence of TGF- β 1 (Fig. 2C). In the culturing dish, only 6% of cells endogenously expressed SNAI1; however, when treated with TGF- β 1, 59% of SW480 cells showed positive immunoreactivity against SNAI1 with loss of CDH1 expression at the cell-cell borders (Fig. 2D) with increased levels of *VIM* expression (Fig. 2E). Moreover, the induction of TGF- β -mediated EMT was confirmed by the finding the SNAI1-positive cells only at the tumor sphere surface (Fig. 2F). Similar results were detected in the experiments using a colorectal CSC differentiation model (unpublished data). Comparative studies of gene expressions of TGF- β receptors and TGF- β -induced EMT in CD133⁺ and CD133⁻ cells were also examined in the other human CRC cell lines; however, we could not find any significant differences as was detected in SW480 cells (data not shown).

SNAI1 mediates the re-acquisition of CSC-like properties in vitro and in vivo. Restoration of SNAI1-expression in CD133⁻ SW480 cells was performed to investigate the impact of EMT on the restoration of CSC-like properties. In SW480 cells,

an increased population of CD133⁺ cells was detected when pSNAI1 was transduced into CD133⁻ SW480 cells (Fig. 3A). The change in the mRNA levels of CDH1 was significant between CD133⁻-EV and CD133⁻-pSNAI1 cells; however, there was no significant change in the mRNA levels of *VIM*, *CDX2* and *MUC2* (Fig. 3B).

Restoration of the stemness was supported by the results of a limiting dilution assay, in which frequency of development of subcutaneous tumors was significantly higher in CD133⁻-pSNAI1 cells than in the tumors derived from CD133⁻-EV cells (Fig. 3C). In addition, transduction of pSNAI1 effectively increased the activities of cell motility, invasion and up-regulated the *MMP2* levels (Fig. 3D-F). In the mouse xenografts derived from CD133⁻-pSNAI1 cells, the cancer cells showed infiltration into the stroma and formed TB-like structures with a high frequency of CD133⁺ cells (Fig. 3G). Furthermore, CD133⁻-pSNAI1 cells showed high TGFBR1 expression and the stromal cells demonstrated SMA expression (Fig. 3G). These findings suggest that transduction of SNAI1 strongly enhances not only the restoration of CSC properties but also the formation of tumor buds.

Induction of SNAI1 at the invasive front correlates with formation of tumor buds and metachronous lymph node metastasis. The obtained data suggested that the mediation by TGF- β and

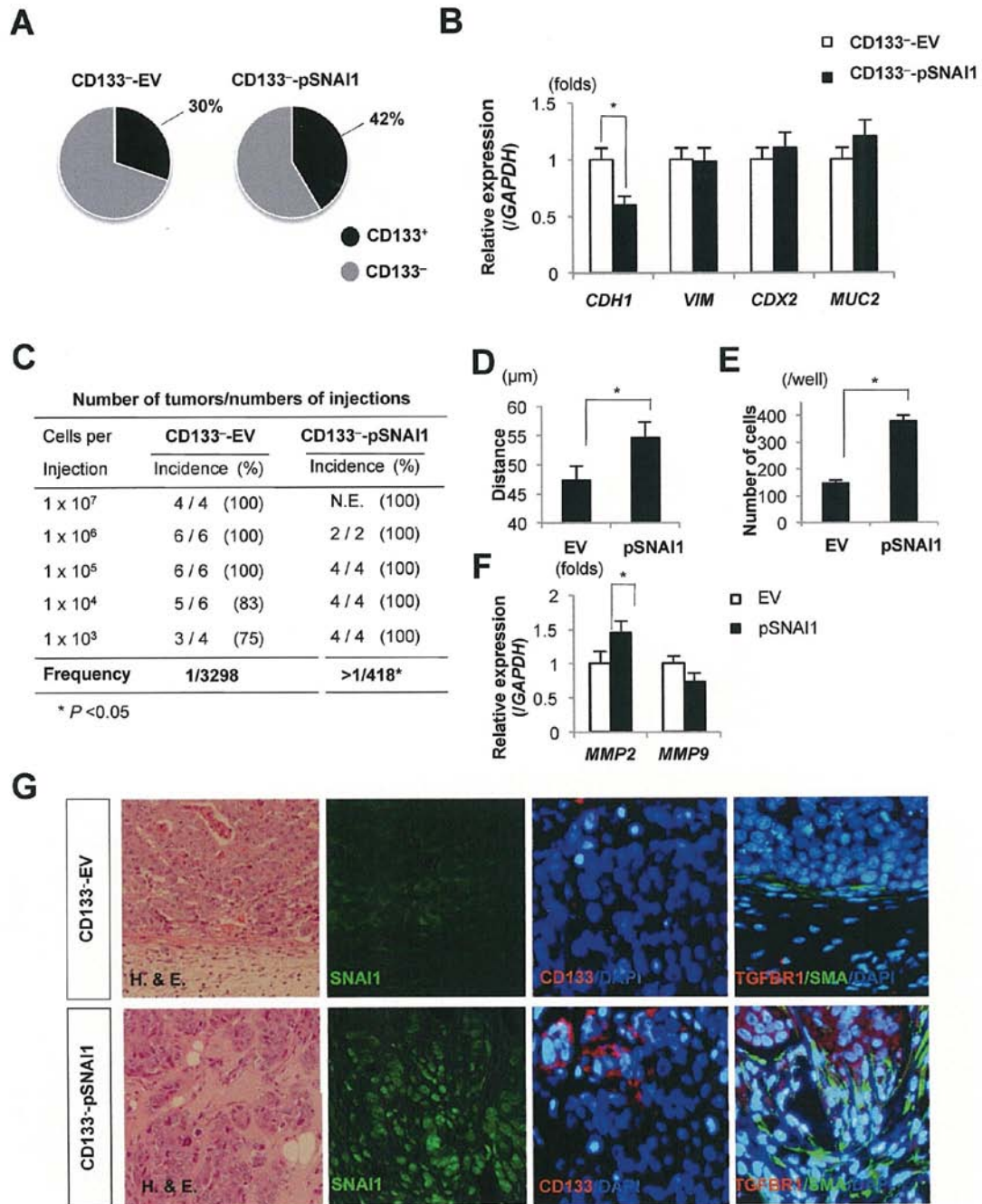


Figure 3. Induction of SNAI1 restores CSC-like properties in SW480 cells. (A), Percentages of CD133⁺ cells in CD133-EV and CD133-pSNAI1 cells 48 h post-transfection. (B), Expressions of EMT (*CDH1* and *vimentin*) and colon markers (*CDX2* and *MUC2*) in CD133-EV and CD133-pSNAI1 cells. (C), Results of limiting dilution assay of CD133-EV and CD133-pSNAI1. Initiating cell frequency was calculated using ELDA as described in Materials and methods. Included in calculation, assumption of 100 CD133-pSNAI1 cells initiate 0 tumor in 4 injections. (D and E), Results of migration assay (D), invasion assay (E) and *MMP2* and *MMP9* expression (F) in CD133-EV and CD133-pSNAI1 cells. (G), Histological examination (H&E) and immunofluorescence of SNAI1, CD133, TGFBR1 and SMA in s.c. xenografts derived from CD133-EV and CD133-pSNAI1 cells. The nuclei were stained with DAPI.

subsequent induction of SNAI1 in CRC cells were necessary for the maintenance of the restoration of CSC-like properties. Therefore, we examined the association of SNAI1 expression and TB formation at the invasive front of 59 cases of stage II CRC. Interestingly, the incidence of TB at the invasive front in CRC cases with metachronous lymph node metastasis was higher than that in those without metachronous lymph node metastasis (Fig. 4A and B). Supporting this, CDX2-positive CRC cells were detected not only in the carcinoma-derived gland structures but also in the budding areas; however, SNAI1-

positive CRC cells were detected only in the budding areas but not in the main tumor (Fig. 4A). These findings suggest the possibility that TB formation at the invasive front is associated with SNAI1-mediated EMT.

Discussion

According to the CSC hypothesis, tumors possess a hierarchical organization of cells, among which a subpopulation of stem-like cells is responsible for sustaining tumor growth

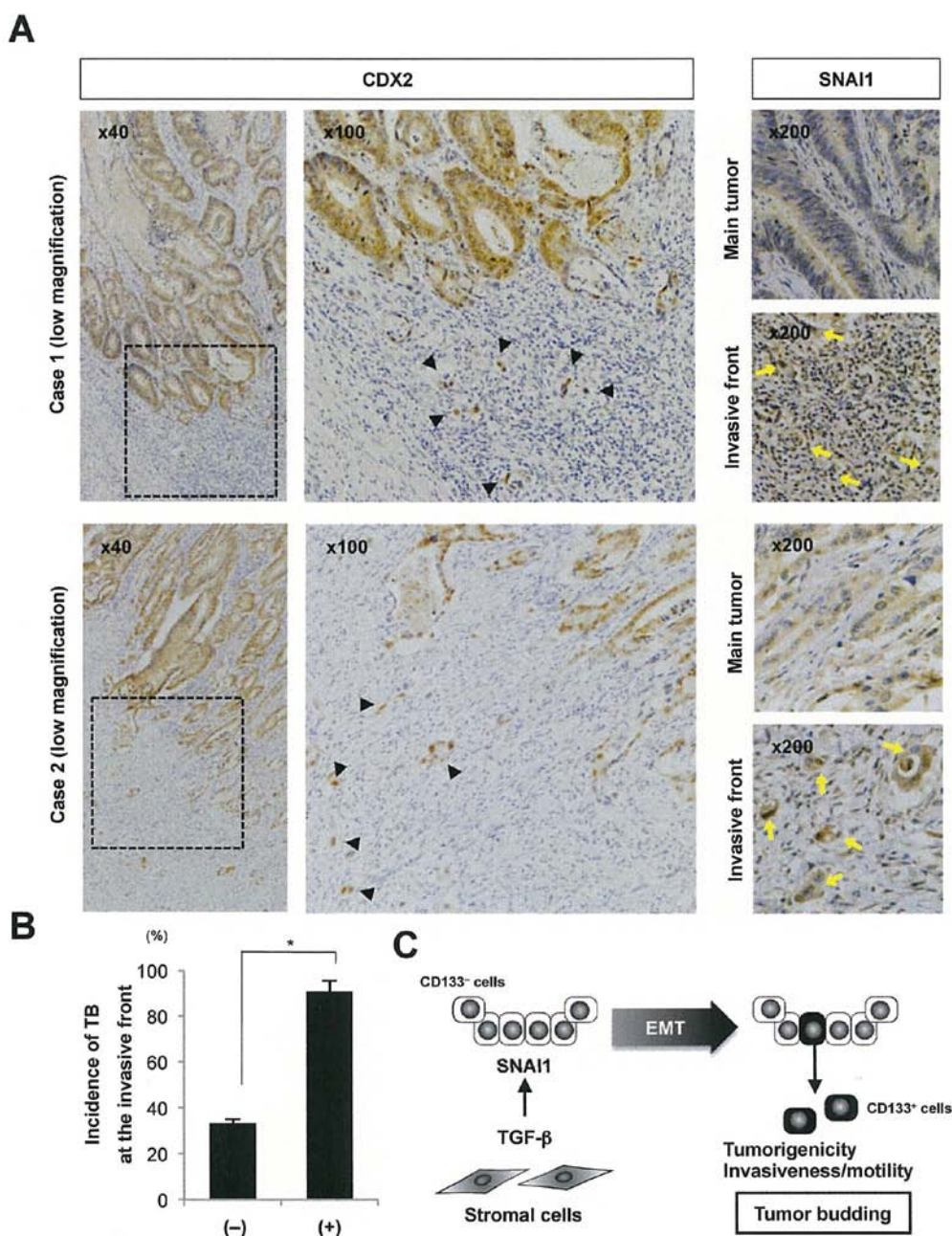


Figure 4. Expression of SNAI1 at the invasive front of CRC correlates with TB and the incidence of lymph node metastasis. (A), Expression of CDX2 and SNAI1 at the invasive front and the main tumor of case 1 (upper panel) and case 2 (lower panel). Arrows indicate representative tumor buds. (B), Incidence of TB at the invasive front of stage II CRC. The incidence of lymph node metastasis was closely correlated with TB at the invasive front. (C), A schematic model of TB induced by TGF- β in CRC. In normal colorectal mucosa, TGF- β supplied from stromal cells maintains stem cells located at the bottom of the epithelial crypt. Also, TGF- β at the invasive front of CRC suppresses the differentiation process by inducing SNAI1-mediated EMT, resulting in restoration of CSC-like properties and formation of TB.

(22,23). In this study, we analyzed the nature of colorectal CSCs to elucidate the relation with TB formation. In SW480 cells, CD133⁺ cells demonstrated high tumorigenicity and pluripotency, whereas CD133⁻ cells did not express the other CSC markers CD44 and Lgr5 in CRC-derived cell lines. In addition, various populations of CD133⁺ cells were detected in CRC-derived cell lines (0.1-22.54%). Nevertheless, in a colorectal CSC differentiation model, transduction of pCDX2 into CD133⁺ SW480 cells effectively decreased CD133 levels and tumorigenic potential. CD133 is a 115-120 kDa five-transmembrane domain glycoprotein that was originally identified as a novel protein specifically localizing in micro-

villi of the apical surface of mouse neuroepithelial cells (24), and the cytoplasmic domain of CD133 can be phosphorylated by Src-family tyrosine kinases (25). Although the biological functions of CD133 are not well understood, the association with the TGF- β signaling pathway and high tumor-forming capability of CD133⁺ SW480 cells strongly support the idea that this glycoprotein would be useful as a molecular target for the diagnosis and treatment of CRC. Thus, we concluded that CD133 is available for the identification of CSCs in SW480 cells.

In this study, we found that CD133⁺ SW480 cells expressed high levels of *SNAI1*, *TGFBR1* and *TGFBR3* transcripts.

Interestingly, we found that treatment with TGF- β 1 up-regulated SNAI1 expression in SW480 cells with the induction of EMT. Of note, the increase in SNAI1 expression was not distributed homogeneously, but the number of SNAI1⁺ SW480 cells was significantly increased in Petri dishes and in tumor spheres in Matrigel. Taken together with the fact that TGF- β 1 restored CD133⁺ SW480 cells, these findings suggested that induction of SNAI1 by TGF- β may be closely related with restoration and maintenance of CSC properties (26). Supporting this idea, transduction of pCDX2 into CD133⁺ SW480 cells effectively suppressed *TGFBR1* and *TGFBR3* expression but treatment with TGF- β restored CD133⁺ SW480 cells and induced EMT. TGF- β did not necessarily induce EMT in the other CRC-derived cell lines, which is probably associated with expression levels of *TGFBR1* and *TGFBR3*. Moreover, transduction of pSNAI1 into CD133⁺ SW480 cells effectively up-regulated CD133⁺ cells with high tumorigenic potential in the mouse xenograft model and simultaneously increased cell motility/invasiveness and *MMP2* expression. Activation of the SMAD signaling by TGF- β directly induces the expression of SNAI1, which subsequently suppresses CHD1 expression by direct binding to the E2-box sequence of the *CDH1* promoter (27). The evidence indicates that TGF- β -mediated maintenance of CSC-like properties may overlap EMT. Based on this body of evidence, we are currently attempting to identify novel molecular markers that are capable of identifying colorectal CSCs.

Finally, we considered that the restoration of stemness could be induced by the surrounding microenvironment in CRC tissues: i.e., TGF- β -induced EMT at the invasive front of CRC is closely correlated with the morphological alteration of tumor cells known as 'TB'. A previous study on patients with pT1 CRC showed that TGF- β -positive cells were observed in 91.7% of patients with presence of TB at the front of invasion, and there was a statistically significant correlation between the presence of lymph node metastasis and the positive expression of TGF- β (28). Furthermore, it has been reported that CD133 expression in colorectal carcinoma is an independent prognostic marker that correlates with low rate of survival (29). In our findings, SNAI1 expression was significantly correlated with TB formation at the invasive front and the incidence of metachronous lymph node metastasis. Consequently, we therefore conclude that TGF- β dissolved in the CRC microenvironment may participate in the SNAI1-induced EMT and restoration of CSC-like properties, which may cause metachronous metastasis in patients with stage II CRC (Fig. 4C). Detection of TB at the invasive front of CRC must be generalized for the accurate evaluation of prognosis of patients with CRC.

Acknowledgements

This work was supported by Grants-in-Aid for Scientific Research (C-19590347 and C-21590370) from the Japan Society for Promotion of Science. Yusra was supported by the scholarship from the Government of the Republic of Indonesia (IP-530).

References

- Imai T: The growth of human carcinoma: a morph anal. *Fukuoka Igaku Zasshi* 45: 72-102, 1954.
- Ueno H, Murphy J, Jass JR, Mochizuki H and Talbot IC: Tumour 'budding' as an index to estimate the potential of aggressiveness in rectal cancer. *Histopathology* 40: 127-132, 2002.
- Shirouzu K, Isomoto H, Morodomi T, Ogata Y, Akagi Y and Kakegawa T: Primary linitis plastica carcinoma of the colon and rectum. *Cancer* 74: 1863-1868, 1994.
- Ueno H, Mochizuki H, Hashiguchi Y, Shimazaki H, Aida S, Hase K, Matsukuma S, Kanai T, Kurihara H, Ozawa K, Yoshimura K and Bekku S: Risk factors for an adverse outcome in early invasive colorectal carcinoma. *Gastroenterology* 127: 385-394, 2004.
- Pardal R, Clarke MF and Morrison SJ: Applying the principles of stem-cell biology to cancer. *Nat Rev Cancer* 3: 895-902, 2003.
- Pheesse TJ and Clarke AR: Normal stem cells in cancer prone epithelial tissues. *Br J Cancer* 100: 221-227, 2009.
- Barker N, van Es JH, Kuipers J, Kujala P, van den Born M, Cozijnsen M, Haegebarth A, Korving J, Begthel H, Peters PJ and Clevers H: Identification of stem cells in small intestine and colon by marker gene *Lgr5*. *Nature* 459: 1003-1007, 2009.
- Sato T, Vries RG, Snippert HJ, van de Wetering M, Barker N, Stange DE, van Es JH, Abo A, Kujala P, Peters PJ and Clevers H: Single *Lgr5* stem cells build crypt-villus structures *in vitro* without a mesenchymal niche. *Nature* 459: 262-265, 2009.
- Vermeulen L, Todaro M, De Sousa Mello F, Sprick MR, Kemper K, Perez Alea M, Richel DJ, Stassi G and Medema JP: Single-cell cloning of colon cancer stem cells reveals a multi-lineage differentiation capacity. *Proc Natl Acad Sci USA* 105: 13427-13432, 2008.
- Yeung TM, Gandhi SC, Wilding JL, Muschel R and Bodmer WF: Cancer stem cells from colorectal cancer-derived cell lines. *Proc Natl Acad Sci USA* 107: 3722-3727, 2010.
- Carpentino JE, Hynes MJ, Appelman HD, Zheng T, Steindler DA, Scott EW and Huang EH: Aldehyde dehydrogenase-expressing colon stem cells contribute to tumorigenesis in the transition from colitis to cancer. *Cancer Res* 69: 8208-8215, 2009.
- O'Brien CA, Pollett A, Gallinger S and Dick JE: A human colon cancer cell capable of initiating tumour growth in immunodeficient mice. *Nature* 445: 106-110, 2007.
- Zhu L, Gibson P, Currie DS, Tong Y, Richardson RJ, Bayazitov IT, Poppleton H, Zakharenko S, Ellison DW and Gilbertson RJ: Prominin 1 marks intestinal stem cells that are susceptible to neoplastic transformation. *Nature* 457: 603-607, 2009.
- Ricci-Vitiani L, Lombardi DG, Pilozzi E, Biffoni M, Todaro M, Peschle C and De Maria R: Identification and expansion of human colon-cancer-initiating cells. *Nature* 445: 111-115, 2007.
- Kojima M, Ishii G, Atsumi N, Fujii S, Saito N and Ochiai A: Immunohistochemical detection of CD133 expression in colorectal cancer: a clinicopathological study. *Cancer Sci* 99: 1578-1583, 2008.
- Horst D, Kriegl L, Engel J, Kirchner T and Jung A: CD133 expression is an independent prognostic marker for low survival in colorectal cancer. *Br J Cancer* 99: 1285-1289, 2008.
- Usami Y, Satake S, Nakayama F, Matsumoto M, Ohnuma L, Komori T, Semba S, Ito A and Yokozaki H: Snail-associated epithelial-mesenchymal transition promotes oesophageal squamous cell carcinoma motility and progression. *J Pathol* 215: 330-339, 2008.
- Hu Y and Smyth GK: ELDA: extreme limiting dilution analysis for comparing depleted and enriched populations in stem cell and other assays. *J Immunol Methods* 347: 70-78, 2009.
- Guo RJ, Suh ER and Lynch JP: The role of Cdx proteins in intestinal development and cancer. *Cancer Biol Ther* 3: 593-601, 2004.
- Watabe T and Miyazono K: Roles of TGF- β family signaling in stem cell renewal and differentiation. *Cell Res* 19: 103-115, 2009.
- Miettinen PJ, Ebner R, Lopez AR and Derynck R: TGF- β induced transdifferentiation of mammary epithelial cells to mesenchymal cells: involvement of type I receptors. *J Cell Biol* 127: 2021-2036, 1994.
- Sting J and Caldas C: Molecular heterogeneity of breast carcinomas and the cancer stem cell hypothesis. *Nat Rev Cancer* 7: 791-799, 2007.
- Visvader JE and Lindeman GJ: Cancer stem cells in solid tumours: accumulating evidence and unresolved questions. *Nat Rev Cancer* 8: 755-768, 2008.
- Weigmann A, Corbeil D, Hellwig A and Huttner WB: Prominin, a novel microvilli-specific polytopic membrane protein of the apical surface of epithelial cells, is target to plasmalemmal protrusions of non-epithelial cells. *Proc Natl Acad Sci USA* 94: 12425-12430, 1997.

25. Boivin D, Labbe D, Fontaine N, Lamy S, Beaulieu E, Gingras D and Béliveau R: The stem cell marker CD133 (prominin-1) is phosphorylated on cytoplasmic tyrosine-828 and tyrosine-852 by Src and Fyn tyrosine kinases. *Biochemistry* 48: 3998-4007, 2009.
26. Peñuelas S, Anido J, Prieto-Sánchez RM, Folch G, Barba I, Cuartas I, García-Dorado D, Poca MA, Sahuquillo J, Baselga J and Seoane J: TGF- β increases glioma-initiating cell self-renewal through the induction of LIF in human glioblastoma. *Cancer Cell* 15: 315-327, 2009.
27. Cano A, Pérez-Moreno MA, Rodrigo I, Locascio A, Blanco MJ, Del Barrio MG, Portillo F and Nieto MA: The transcription factor Snail controls epithelial-mesenchymal transitions by repressing E-cadherin expression. *Nat Cell Biol* 2: 76-83, 2000.
28. Guzinska-Ustymowicz K and Kemon A: Transforming growth factor beta can be a parameter of aggressiveness of pT1 colorectal cancer. *World J Gastroenterol* 11: 1193-1195, 2005.
29. Horst D, Scheel SK, Liebmann S, Neumann J, Maatz S, Kirchner T and Jung A: The cancer stem cell marker CD133 has high prognostic impact but unknown functional relevance for the metastasis of human colon cancer. *J Pathol* 219: 427-434, 2009.